# AIAA 2005 - 1042

COMPUTATIONAL FLUID DYNAMICS STUDY OF TURBULANCE MODELING FOR AN OGIVE USING COBALT FLOW SOLVER AND A 2^N TREE-BASED CARTESIAN GRID GENERATOR

D.V. Grove
Naval Air Systems Command, Patuxent River MD

Z.J. Wang
Iowa State University, Ames IA
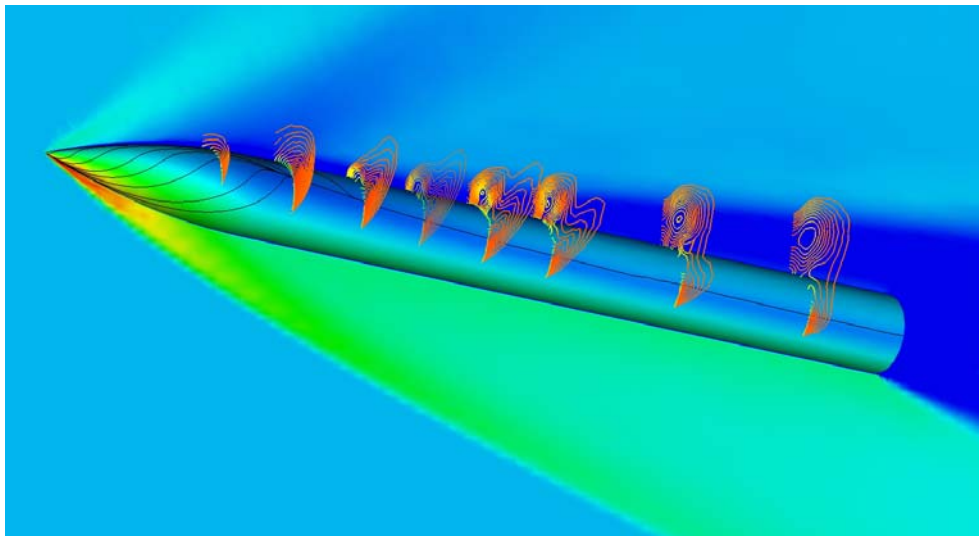
43rd AIAA Aerospace Sciences Meeting & Exhibit
10 –13 January 2005
Reno, NV

Computational Fluid Dynamics Study Of Turbulence Modeling For An Ogive Using Cobalt Flow Solver And A 2^n Tree-Based Cartesian Grid Generator

Darren. V. Grove[*]

Naval Air Systems Command, Patuxent River, MD 20670

grovedv@navair.navy.mil

Z.J Wang[+]

Iowa State University, Ames, IA

zjw@egr.msu.edu

Abstract

A 2^n tree-based Cartesian grid generation method has been developed recently for complex geometries to simulate viscous flows. The "viscous" Cartesian grid is capable of resolving boundary layers with high-aspect ratio projected viscous layer grids. Compared with an Octree data structure, the 2^n tree data structure supports anisotropic grid adaptations in any of the coordinate directions in an arbitrary manner. This capability enables flow features such as shocks, shear layers, and wakes to be resolved very efficiently. In this paper, steady-state Navier-Stokes Computational Fluid Dynamics (CFD) analyses were performed on a cylindrical body Ogive using five different turbulence models in the commercial flow solver Cobalt with the 2^n based Cartesian grid generator. Turbulence models tested were the Spalart-Allmaras (SA), Menter-Shear-Stress Transport (SST), coupled Detached Eddy Simulation – Spalart-Allmaras (DES-SA), coupled Detached Eddy Simulation - Shear Stress Transport (DES-SST), and the κ-ω model. The geometry model consisted of a 3-caliber nose with a cubic profile followed by a 10 caliber cylindrical body. Surface pressures and off body vortex flows were computed and compared to well documented experimental results for a test case at Mach 2.4 and 14° Angle-Of-Attack (AOA). Overall results showed that all turbulence models compared well with experimental with κ-ω giving the best results.

I. Introduction

Unstructured Computational Fluid Dynamics (CFD) has emerged as a critical technology for the design of current and future weapon systems. Influencing factors like advancement in computer technology, budgetary reductions, and limited experimental testing have served to focus emphasis on the development and validation of computational predictive methods. There are many types of unstructured grids currently in use by CFD researchers, which include triangular and tetrahedral grids[1-5], quadrilateral or hexahedral grids[6], prismatic girds[7], or mixed grids[8-9]. One of the most appealing artifacts of the unstructured grid is the ease in which the grid can be adapted to complex flow features like shocks and highly unsteady flow. In the past 10 years significant progress has been made in predicting turbulent airflows such as shock induced separation around wings, or vortical flows off the forebodies of combat air vehicles and missiles.

---

* Aerospace Engineer, NAVAIR, Bldg 2187 Suite 1320-D4, 48110 Shaw Road Patuxent River MD 20670, Senior Member AIAA
+ Associate Professor, Department of Aerospace Engineering, Associate Fellow AIAA

In addition to the advancements in turbulence modeling, significant improvement and new techniques have emerged for grid generation. One such technique is the use of a 2^n tree-based adaptive Cartesian grid generation method for viscous flows. The Navy owned grid generator NavCart, formally CFD-Viscart but modified by internal Navy funds, was used to generate the volume grids. This unstructured grid-based CFD method generates volume meshes by first using a recursive cell-subdivision technique and then proceeds to develop the surface mesh by projecting each front node to the surface in a normal direction[10]. Viscous layers are added by a user specified normal spacing and number of layers parameter. The layers may be added by geometric growth rate or by hyperbolic stretching.

In this paper, we attempt to demonstrate the use of multiple turbulence models using the flow solver Cobalt[11] with the 2^n tree-based data Cartesian grid generation method on a well document Ogive case[12]. The approach of this study was to apply Navier-Stokes computational techniques to a complex flow field with highly separated flow for a missile shape to evaluate turbulence modeling technology with the NavCart grid generator. The overall goal was to compare which turbulence model could best match the experimental data.

II. Test Case & Conditions

The model in this test case is shown in Figure 1. It consists of a 3-caliber nose having a cubic profile followed by a 10-caliber cylindrical section of diameter 3.7 inches. The nose profile is similar to a tangent-ogive and is given by the following profile[13]:

$$r/D = -0.002615*(x/D)^3 - 0.039867(x/D)^2 + 0.30984(x/D)$$

where r is the nose radius at a distance x from the apex and D is the diameter.

Experimental data were taken in the 3ft x 4ft High Supersonic Speed Tunnel (HSST) at the Defense Research Agency (DRA), Bedford, UK. The test case conditions chosen for this study were freestream Mach=2.5, alpha=14°, and Re=4.0×10^6/ft that showed exceptional repeatability as shown in Figure 2. A freestream total pressure $P_{t\infty}$ = 6.092 psi (42kpa) and a freestream total temperature $T_{t\infty}$ = 554.4 °R (308 K) was recorded in the test section.

III. Computational Technique

The flow solver Cobalt of Cobalt Solutions LLC was used for this test case. Cobalt is a finite volume, cell-centered, second-order accurate in space and time unstructured Euler/Navier-Stokes flow solver. The technique used for this study was to: 1) generate an initial viscous grid using the NavCart grid generator; 2) run a quasi steady-state solution to convergence; 3) read the grid and solution back into NavCart and use its solution-based adaptive module to adapt on the total pressure gradients; 4) rerun the new denser grid; 5) repeat this process until the solution showed no changes with grid density, i.e., grid independency; and 6) using the final grid, change the turbulence model in the Cobalt input file and run to convergence. For the DES-SST and DES-SA (Reynolds-averaged Navier-Stokes and Large Eddy Simulations hybrid models) simulations, a time-accurate solution was run and time averaged forces and moments were used in the plots. A converged solution for Cobalt steady-state computations is defined by little to no change in the forces and moments over a range of cycles, typically 200 is sufficient. A plot of forces and moments for the final grid (level 4) Spalart-Allmaras solution is shown in Figure 2. For no specific reason, the Spalart-Allmaras turbulence model was first chosen to run the grids through 4 levels of adaptations until grid independency was achieved. A cut plane along Z=0.0 for the initial grid and 4 levels after adaptation on the solutions are shown in Figure 3.

IV. Viscous Grid Generation & Dependency

The NavCart 2^n tree-based adaptive Cartesian grid generator was used to mesh the volume grid of the Ogive. NavCart is capable of generating both inviscid and viscous type volume meshes. For viscous type volumes, it is capable of resolving boundary layers with high-aspect ratios. In addition, the 2^n tree supports binary, Quadtree, and Octree type of subdivisions, and therefore allows the adaptive Cartesian grid to be refined in a non-isotropic manner. The use of anisotropic grid adaptation (vs. isotropic grid adaptation) offers the potential of dramatically reduction in the total number of cells to achieve a given level of solution accuracy since most high-gradient flow features like shock waves, slip lines, vortex sheets, and wakes are anisotropic.

An initial plot3d surface mesh of the Ogive was generated with Gridgen. The plot3d file was then read into NavCart, which automatically triangulated the plot3d surface mesh to form a watertight unstructured mesh. The viscous Cartesian grid approach was used to generate the volume mesh. This approach consists of five basic functions including 1) Cartesian grid generation, 2) Cartesian grid front generation and smoothing, 3) projection of the Cartesian front to the body surface, 4) geometric feature preservation, and 5) surface grid smoothing and layer grid generation. These functions are explained in detail in Reference 10.

For this study, an initial volume grid (level 1) of 165,448 cells was generated with a viscous layer consisting of 15 layers as shown in Figure 4. A 0.5-inch boundary layer thickness was set as the normal distance off the surface. A hyperbolic stretching function was use with the first point off the surface set at 0.001 inch, giving an average Y^+ value of 1.15 when run with the Cobalt flow solver. The initial mesh took 8 seconds to generate using a dual Xeon 2.4GHz computer. All solutions were run in parallel using 12 CPU's on NAVAIR Store Separation Branches Linux cluster. The cluster consists of 32 CPU's running at 2.4GHz using the Red Hat 7.3 OS. The initial grid was run for 1000 Cycles then read back into NavCart and the adaptation module was used to adapt on the total and static pressure gradients. This process was repeated until no changes in computed surface pressure coefficients were seen, i.e., grid independency was achieved. Each steady-state solution was run to 1000 cycles and all went to convergence. A table of flow solver time (seconds) vs. each turbulence model and grid density levels is shown in Table 1.

V. Time Accurate Solutions

Since the Detached Eddy Simulation turbulence model was formulated to better capture off body large eddies, time accurate solutions were performed with the DES-SA and DES-SST turbulence models. A time step of .0001069 was used for the simulations. The time step was derived by first finding a characteristic time step d/V_∞. The physical time step needs to be some small multiple of the characteristic time step. A 0.02 multiplier was used giving the physical time step of 0.0001069 for each simulation. Each simulation was run for 5612 cycles giving a 0.5 second physical solution time. Time-averaged surface pressure coefficients were compute and compared to wind tunnel data.

VI. Forces and Moments

All forces and moments were for the 13D body. Reference area is the nominal base area, $\pi d^2/4$, where the nominal diameter d is 3.7 inches. Reference length for C_m, C_l, C_n equals the nominal diameter. The moments C_m, C_l, C_n was taken about the nose (X=0).

VII. Results

Five turbulence models were tested including the Spalart-Allmaras (SA), Menter-Shear-Stress Transport (SST), coupled Detached Eddy Simulation - Spalart-Allmaras (DES-SA), coupled Detached Eddy Simulation - Shear Stress Transport (DES-SST), and the k-w model. Comparison of computed vs. experimental surface pressure coefficients were take at x/D= 2.4, 3.5, 4.5, 5.5, 6.5, 7.5, 9.5, and 11.5 where x is the axial direction and D is the Ogive diameter. Figures 5 thru 9 show the results for each turbulence model as indicated at the bottom of the figure. Overall, each turbulence model does a good job at predicting the Cp for x/D= 2.4, 3.5, 4.5, 5.5, 9.5, and 11.5. However all turbulence models over predict the surface pressures around Phi=100 and 150 degrees for x/D= 6.5 and 7.5 as shown in figure 10. Maybe more grid refinement in these areas is needed. But for this study, the message indicates that the more sophisticated two-equation turbulence models do not provide a clear advantage over the less sophisticated one-equation models.

Force and moments are compared in Table 2 for computed vs. experimental. All turbulence models predicted within 1.05% of the normal force and 0.88% of the pitching moment. If one had to base the best turbulence model on this table, it would be the κ-ω with a .58% difference in CN (normal force coefficient) and .78% difference in Cm (pitching moment coefficient). However, any one of the models could be used for this type of simulation with a high degree of confidence.

VIII. Conclusions

The NavCart 2^n tree-based adaptive Cartesian grid generator has been tested with viscous flow. A well-documented test case was performed using the Cobalt Solutions LLC flow solver COBALT. Overall, good agreement of the surface pressure coefficients was achieved with slight over prediction at Phi = 100 and 150 degrees at x/D=6.5.and 7.5. All turbulence models predicted within 1.05% of the normal force coefficient and .88% of the pitching moment coefficient. The solution based adaptation method has shown to be very effective in capturing shock waves and complex vortex structures. Overall all turbulence models show good results with the κ-ω predicting slightly better then the others in force and moments with a marginal increase in computer time.

IV. Acknowledgment

X. References

[1] Barth, T.J., and Frederickson, P.O., Higher–Order Solution of the Euler Equations on Unstructured Grids Using Quadratic Reconstruction, AIAAPaper 90–0013, 1990.

[2] Batina, J.T., Unsteady Euler Algorithm with Unstructured Dynamic Mesh for Complex Aircraft Aerodynamic Analysis, AIAA Journal, vol. 29, pp.327–333, 1991.

[3] Venkatakrishnan, V., Convergence to Steady State Solutions of the Euler Equations on Unstructured Grids with Limiters," J. Comput. Phys., vol. 118, 1995, pp. 120–130.

[4] Anderson, W.K. and Bonhaus, D.L., An Implicit Upwind Algorithm for Computing Turbulent Flows on Unstructured Grids, Computers Fluids, 23 (1994), pp. 1–21.

[5] Connell, S.D. and Holmes, D.G., A 3D Unstructured Adaptive Multigrid Scheme for the Euler Equations, AIAA paper 93–3339–CP, 1993.

[6] Schneiders, R., "Automatic Generation of Hexahedral Finite Element Meshes," in Proceedings of 4th International Meshing Roundtable '95, October 1995, Albuquerque, NM.

[7] Nakahashi, K., "Adaptive–Prismatic–Grid Method for External Viscous Flow Computations," in Proceedings of 11th AIAA Computational Fluid Dynamics Conference, July 1993, Orlando, FL. AIAA–93–3314–CP.

[8] Kallinderis, Y., Khawaja, A. and McMorris, H., "Hybrid Prismatic/Tetrahedral Grid Generation for Complex Geometries," AIAA Paper No. 95–0210, 1995.

[9] Coirier, W.J. and Jorgenson, P.C.E., "A Mixed Volume Grid Approach for the Euler and Navier–Stokes Equations," AIAA Paper No. 96–0762,1996.

[10] Wang, Z.J. and Chen, R.F. "Anisotropic Solution-Adaptive Viscous Cartesian Grid Method for Turbulent Flow Simulation", *AIAA Journal*, Vol. 40, No. 10, pp. 1969-1978, 2002.

[11] Bob Tomaro, William Strang, Ken Wertzler, Jim Forsythe, "Cobalt Users Manual Version 3", Cobalt Solutions, LLC.

[12] Walter Sturek, U.S ARL, APG, Trever Birch, DRA UK, Marc Lauzon, DRE, Valcartier CA, Clinton Housh, NAWC, China Lake, CA, Joe Manter, AFRL Wright-Patterson AFB, OH, Eswar Josyula, AFRL Wright-Patterson AFB, OH, Bharat Soni, MSU, Starkville, MS, "The Application of CFD to Prediction of Missile Body Vortices", 35th Aerospace Sciences Meeting & Exhibit, AIAA 97-0637, 1997.

13. Trevor Birch, DRA UK, "KTA-2-12 The Application of CFD to the Prediction of Missile Body Vortices, Final Report", The Technical Cooperation Program, Subgroup W, Conventional Weapons Technology, Appendix B, pp. 2 June 1997.
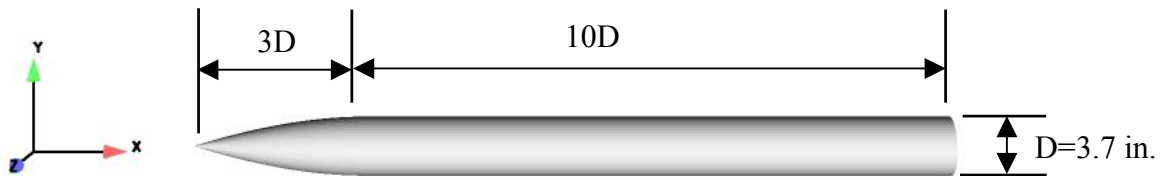
Figure 1. Side view of 13D Ogive with axes.

Computed Force Vs Number of Cycles
Turb Model = SA, M=2.5, AoA=14, Re=4.0e6
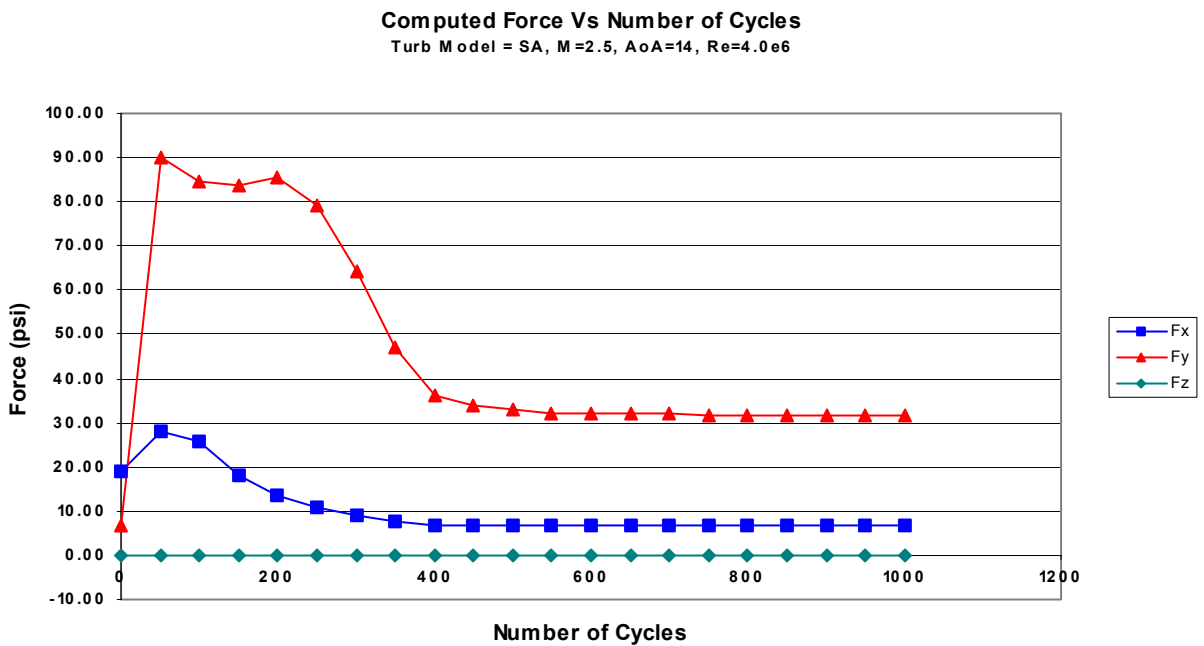
**Figure 2. Force vs. number of Cycles for the Spalart-Allmaras turbulence model.**
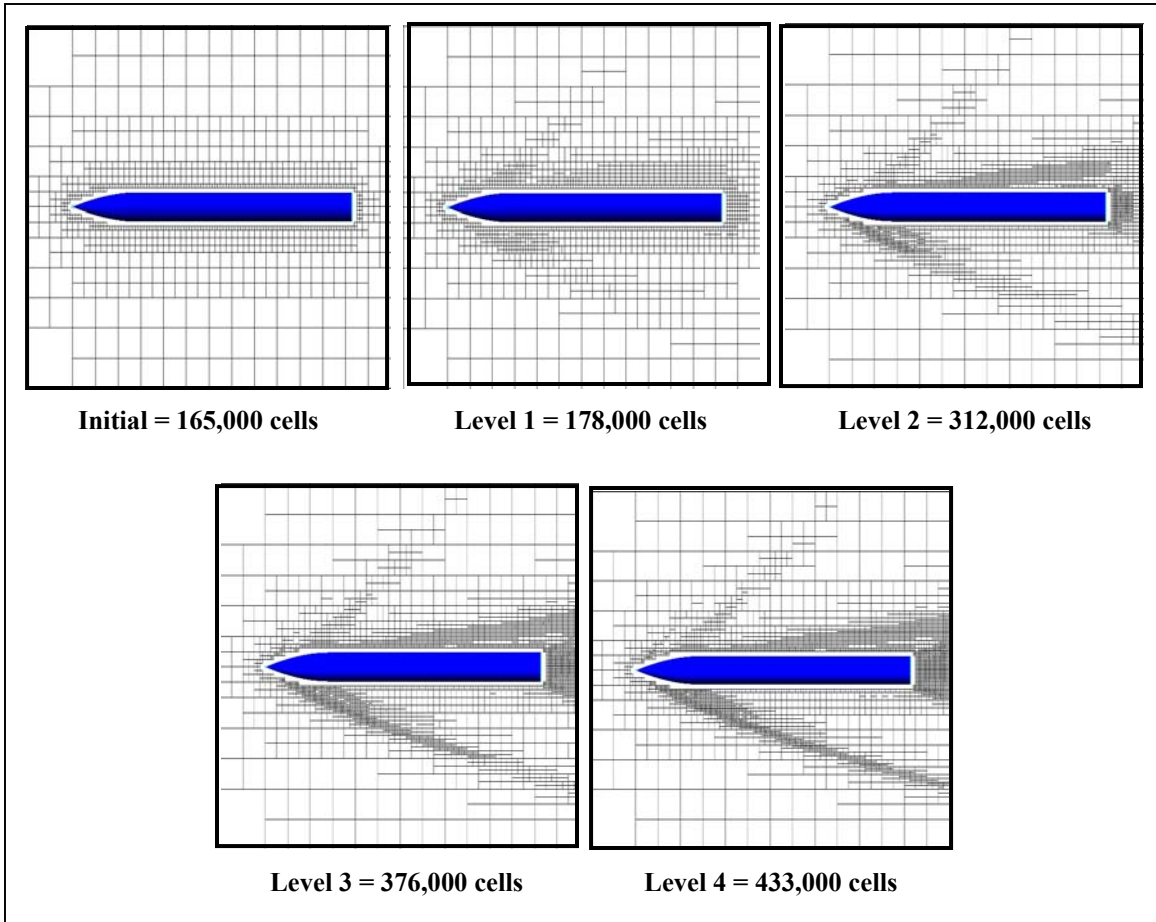
Figure 3. The initial and 4 levels of Solution-Adapted grids using 2^n Tree.
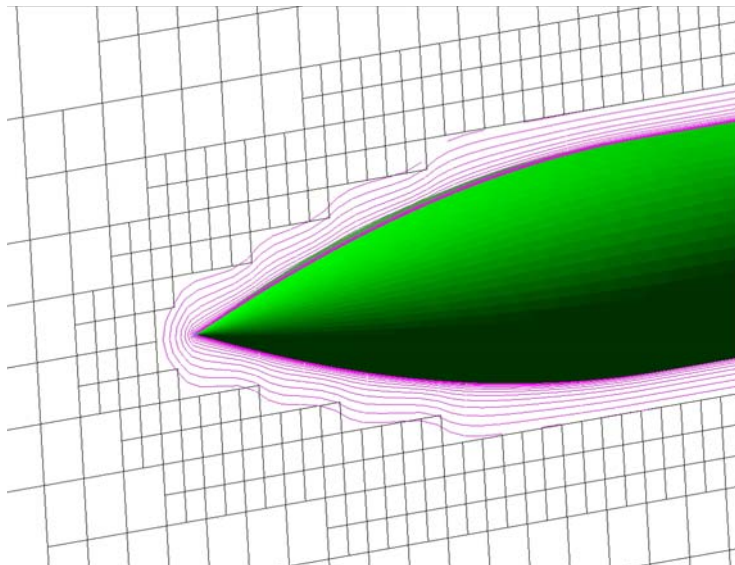
Figure 4. Viscous layers around Ogive nose using hyperbolic stretching.

Grid	SA	kω	SST
Initial	30.8 min.	NA	NA
Level (1)	34.9 min.	NA	NA
Level (2)	78.15 min.	NA	NA
Level (3)	98.4 min.	NA	NA
Level (4)	104.8 min.	115.7 min.	98.0 min.

**Table 1. Time (seconds) to run 1000 Cycles vs. Turbulence models per grid level**
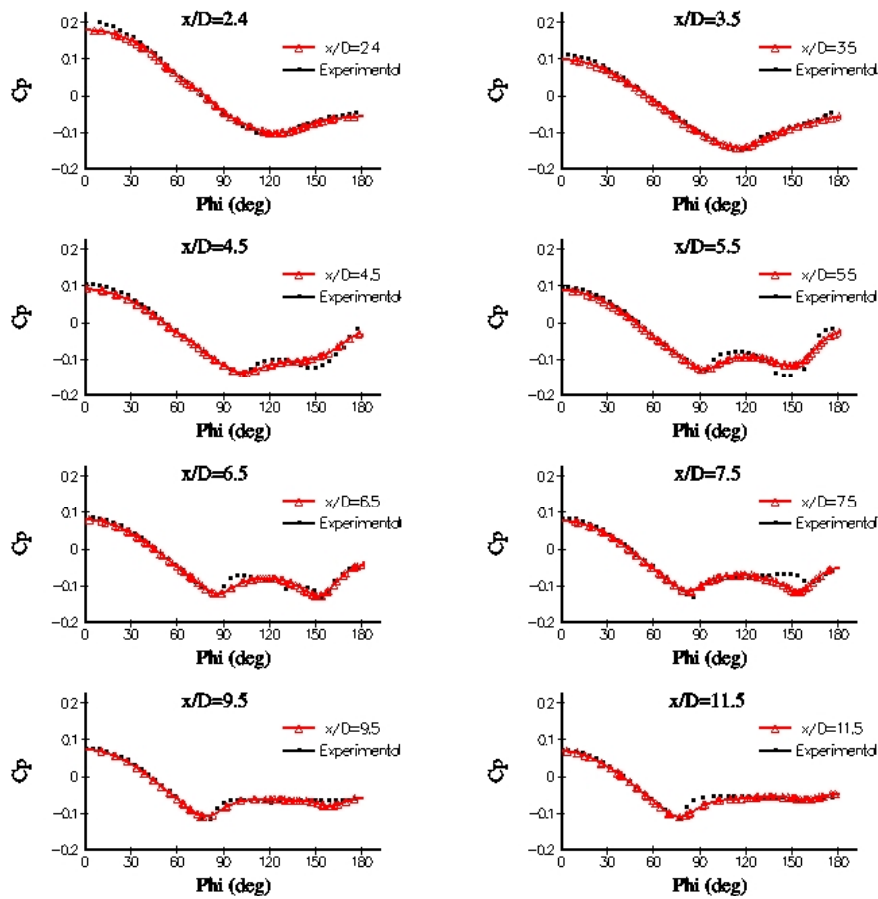
Figure 5. Plots of Cp vs. Phi (deg) at various x/D locations for the Spilart-Allmaras turbulence model.
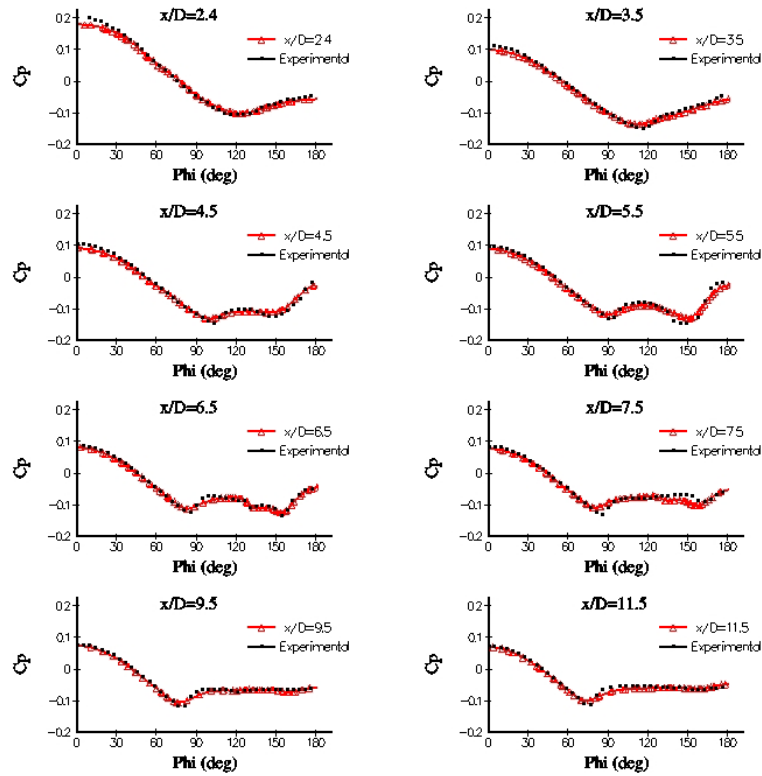
Figure 6. Plots of Cp vs. Phi (deg) at various x/D locations for the DES – Spalart-Allmaras turbulence
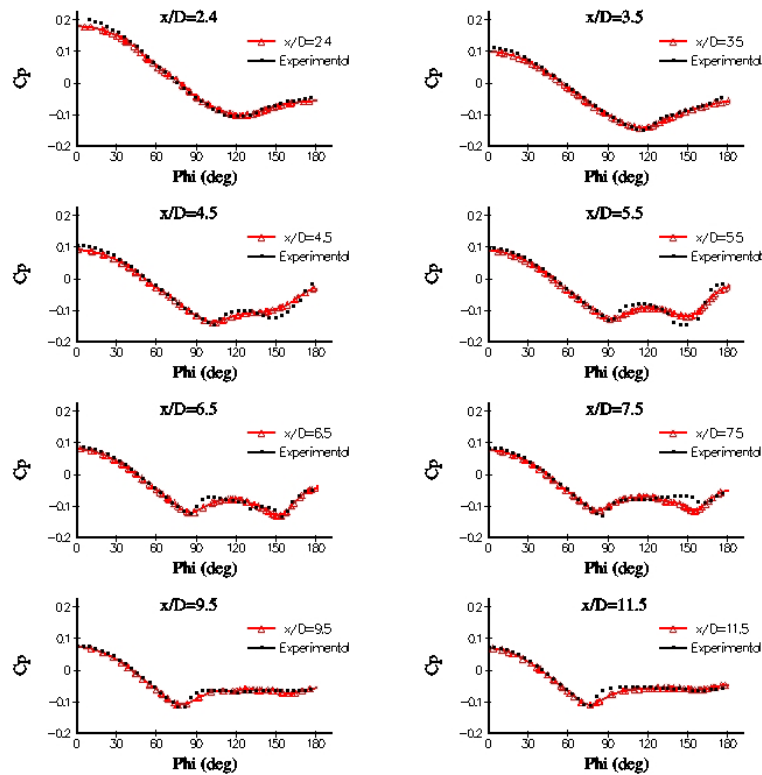

**Figure 7. Plots of Cp vs. Phi (deg) at various x/D locations for the SST turbulence model.**
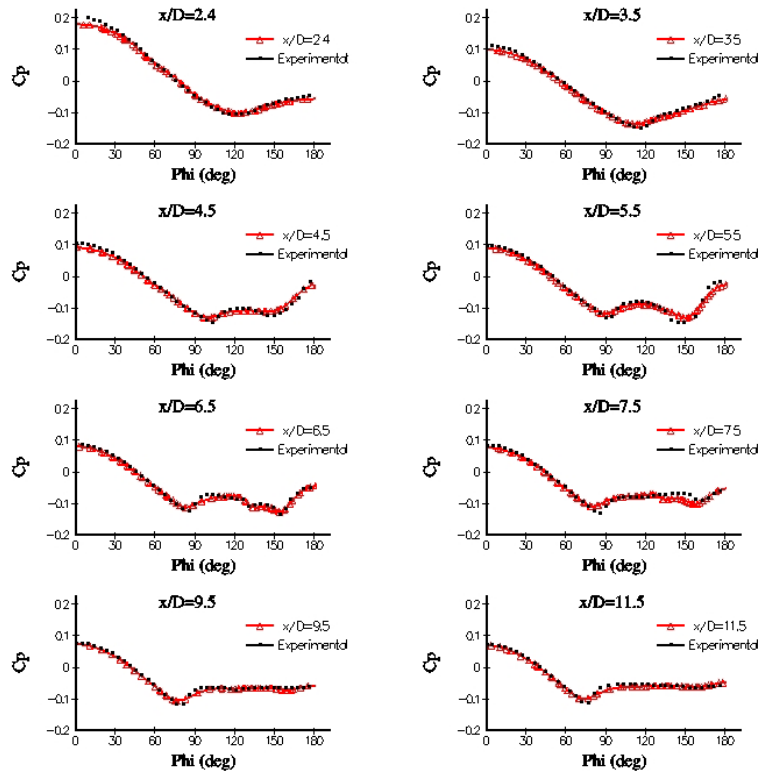
Figure 8. Plots of Cp vs. Phi (deg) at various x/D locations for the DES-SST turbulence model.
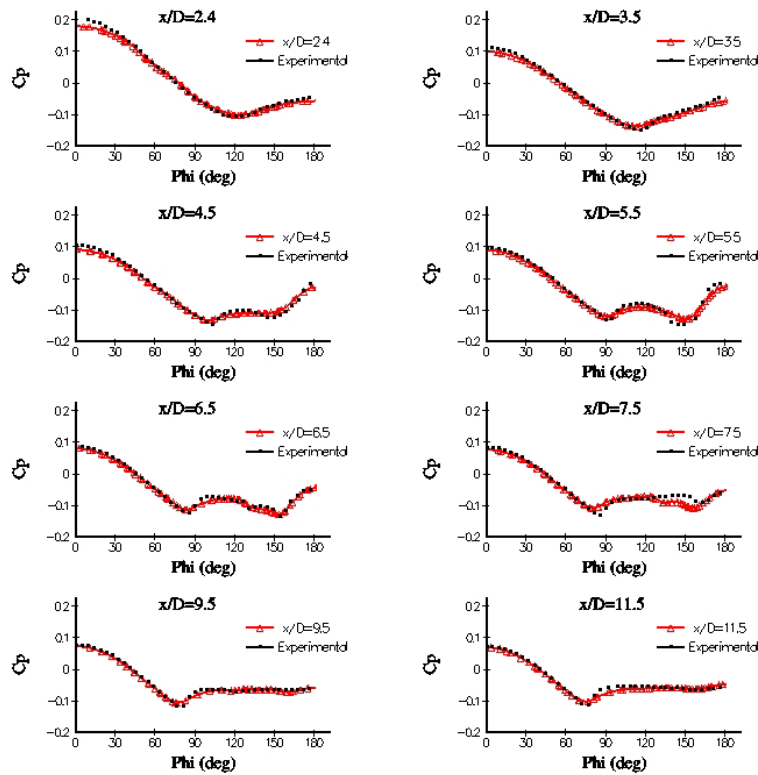

Figure 9. Plots of Cp vs. Phi (deg) at various x/D locations for the κ-ω turbulence model.

x/D=7.5
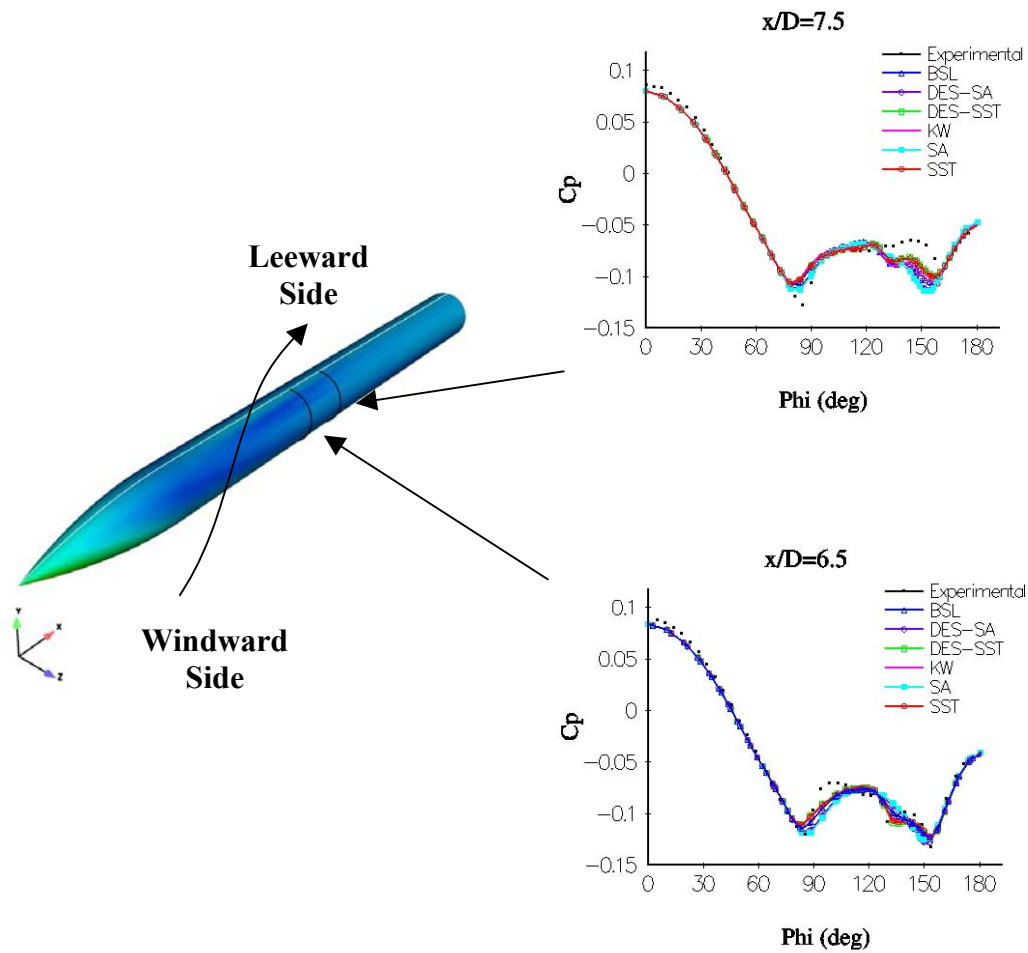
x/D=6.5

Figure 10. Ogive showing wind flow direction and Plots of Cp vs. Phi (deg) at x/D= 6.5 & 7.5 for all turbulence models.

	Comp Cn	Exp Cn	% diff	Comp Cm	Exp Cm	% diff	Sec/Iter	Time (min)
DES-SST	1.9	1.91	0.52	-10.327	-10.24	0.85	NA	NA
DES-SA	1.89	1.91	1.05	-10.21	-10.24	0.29	NA	NA
SA	1.89	1.91	1.05	-10.27	-10.24	0.29	6.01	104.8
SST	1.9	1.91	0.52	-10.33	-10.24	0.88	5.67	98
KW	1.9	1.91	0.52	-10.32	-10.24	0.78	6.7	115.7

Table 2. Comparison of Experiment and Computed normal force and pitching moment